A Mesoporous Template Route to the Low-Temperature Preparation of Efficient Green Light Emitting Zn_2SiO_4:Mn Phosphors

Liangming Xiong, Jianlin Shi,* Jinlou Gu, Liang Li, Weimin Huang, Jianhua Gao, and Meiling Ruan

State Key Laboratory of High Performance Ceramics and Superfine Microstructure, Shanghai Institute of Ceramics, Chinese Academy of Sciences, Shanghai 200050, People's Republic of China

Received: September 26, 2004

Green light emitting Zn_2SiO_4:Mn phosphors have been prepared via a low-temperature solid-state reaction using mesoporous silica SBA-15 template. This mesoporous silica template method features low-temperature formation of phosphors and easy doping. The structure and morphology of the phosphors were characterized by XRD, SEM, TEM, and N_2 adsorption/desorption techniques, which confirmed the single crystallinity, ordered mesostructure, closed pore channels, and elongated ropelike morphology. The luminescent properties were examined by photoluminescence spectroscopy at room temperature, and the results of fluorescence decay time measurements show non-single-exponential decay behavior and a decrease of the decay time with an increase of the Mn concentration.

Introduction

Over the past few years, a family of periodic mesoporous silica materials with high surface area have received much attention because of their useful catalytic properties, catalyst supports, and current or potential applications as adsorbents, hosts, and templates for nanocasting and preparing one-dimensional nanostructures.[1] As hosts or templates, however, mesoporous silica materials act only as a passive stiff mold to shape the heterogeneous nanostructures and seldom take part in the chemosynthesis of functional or nanostructured species, though the silanol groups on the wall have been exploited to chemically modify the mesopores.[2] Using mesoporous silica as an active template is practical, with possibly even broader applications, for the preparation of silicates supported on a mesoporous silica framework with remarkable optical and catalytic properties.[3,4] For example, recently, our research group has reported the preparation of enhanced luminescent $Eu_8(SiO_4)_6$ nanorods using Eu-doped MCM-41 via solid-state reaction at around 1273 K.[3]

On the other hand, the interest in making flat panel displays more commercially feasible has triggered a wide range of subsequent investigations on the luminescent properties of inorganic phosphors.[5,6] Among the known inorganic phosphors, manganese-doped zinc silicate (Zn_2SiO_4:Mn) is an efficient green emitting phosphor widely used in cathode ray tubes (CRTs), fluorescent lamps, and plasma display panels (PDPs) thanks to its high luminescent efficiency and chemical stability, and it also presents the advantage of highly saturated color.[7] Recently, Zn_2SiO_4:Mn was found to be appropriate for low-voltage radiography and fluoroscopy, especially in mammographic applications.[8] Conventionally, the Mn^{2+}-doped Zn_2SiO_4 phosphors are fabricated mainly by solid-state reaction (SSR) of starting powders, e.g., ZnO, SiO_2, and $MnCO_3$, at about 1200 °C or even higher.[5,9] Despite the simplicity of this method, the high firing temperatures required and the subsequent grinding and ball milling processes make it rather difficult to control the particle shape and sizes, on which the luminescent properties of phosphors strongly depend.[10] To improve its physical, chemical, and photoluminescent properties, extensive research in searching for new synthetic techniques and optimization of the host and activator species has been carried out, and some other new preparation approaches, such as hydrothermal, sol−gel, coprecipitation, and fume pyrolysis methods, have been proposed.[6,11,12] In some of these new preparation approaches, low-temperature synthesis and easy doping can be achieved; however, the chemical stoichiometry and crystallinity of the synthesized materials still need to be improved, which also strongly affects the luminescent properties of phosphors. To achieve high-definition color PDPs, however, a high quantum efficiency, good color purity, and proper decay time are required for phosphors.

In the present work, we report the preparation of well-crystallized Zn_2SiO_4:Mn phosphors via solid-state reaction at as low as 850 °C by using mesoporous silica SBA-15 as an active template. This synthesis route of Zn_2SiO_4:Mn phosphors using mesoporous silica exhibits a significant advance in facilitating homogeneous doping, enhancing their luminescent properties, and lowering the firing temperatures that are required in the conventional solid-state reaction method.

Experimental Section

The mesoporous silica SBA-15 was synthesized according to the reported procedure[13] in the following manner: an 8.0 g aliquot of the triblock copolymer $EO_{20}PO_{70}EO_{20}$ (Pluronic P123, BASF) was dissolved in 60 g of distilled water and 240 g of 2 M HCl solution under stirring at about 40 °C, and 17 g of tetraethoxysilane (TEOS) was added to this homogeneous solution under stirring at 40 °C for 24 h. This mixture was then heated at 100 °C for 2 days without stirring. The resulting white solid was filtered on a Buchner filter, washed repeatedly with water, dried at 60 °C, and finally calcinated in air at 530 °C for 6 h to remove the surfactant template.

* To whom correspondence should be addressed. E-mail: jlshi@sunm.shcnc.ac.cn.

10.1021/jp045630s CCC: $30.25
Published on Web 12/17/2004

In the typical synthesis of Zn_2SiO_4:Mn phosphor, a calcinated sample of SBA-15 was stirred overnight in ethanolic manganese-(II) acetate tetrahydrate and zinc acetate dihydrate solution [approximately 61 mg of SBA-15 per 0.08 mmol of manganese-(II) salt and 1.92 mmol of zinc salt per 10 mL of ethanol for a $Zn_{2-x}Mn_xSiO_4$ ($x = 0.08$) sample]. The ethanol suspension was dried at room temperature in a strong flow of air in a fume cupboard while maintaining continuous stirring to form the precursor $Zn(AC)_2$&$Mn(AC)_2$-supported SBA-15. The dry precursor was calcinated in a flow of N_2 atmosphere in stages, at 530 °C for 1 h and at 650−850 °C for 3 h. In this experiment, zinc nitrate hexahydrate was an alternative for zinc acetate to be used as the Zn^{2+} source, and other phosphors with different amounts of Mn doping levels were obtained with the same method but varying both zinc salt and manganese salt concentrations. The as-prepared phosphors at different manganese doping levels are denoted *x*M-ZS, where *x* stands for the Mn^{2+}/Si^{4+} molar ratio percentage used (e.g., 0, 2, 5, 8, and 12), and the samples 8M-ZS prepared using zinc acetate and zinc nitrate as the zinc source are named 8M-ZS(A) and 8M-ZS(N), respectively. For the purpose of comparison, 8 mol % Mn-doped Zn_2SiO_4 phosphor was prepared by the conventional solid-state reaction method at 1250 °C for 4 h according to the literature,[5] and is denoted sample CSSR.

The XRD patterns of the as-prepared samples were recorded on a Rigaku D/Max-2550V X-ray diffractometer with a Cu target (40 kV, 40 mA). Field emission scanning electron microscopy (FE-SEM) measurements were performed on a JSM-6700F field emission scanning electron microscope. Transmission electron microscopy (TEM) and selected area electron diffraction (SAED) analysis were conducted with a JEM2010 electron microscope operated at 200 kV. N_2 adsorption and desorption isotherms were obtained on a Micromiritics Tristar 3000 analyzer at 77.35 K. Photoluminescence (PL) spectra and decay kinetics of the green emission of the prepared samples were measured on a Shimadzu RF-5301 spectrofluorophotometer with a slit width of 1.5 nm and a Jobm Yvon Fluorolog-3 at room temperature, respectively.

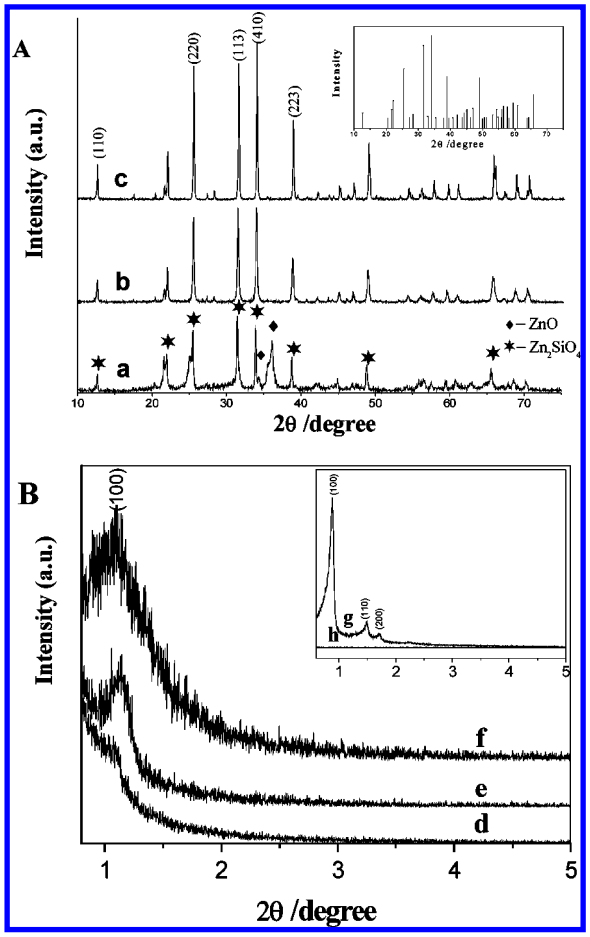

Figure 1. (A) wide-angle XRD patterns of (a) sample 8M-ZS(A) fired at 750 °C, (b) sample 8M-ZS(A) fired at 850 °C, and (c) sample CSSR fired at 1250 °C. Inset in (A): standard pattern reported by JCPDS Card No. 08-0492 for willemite, syn. (B) Low-angle XRD patterns of (d) sample 0M-ZS, (e) sample 8M-ZS(N), and (f) sample 8M-ZS(A) fired at 850 °C. Inset in (B): low-angle XRD patterns of (g) the mesoporous silica SBA-15 template and (h) the reference sample CSSR.

Results and Discussion

Figure 1A shows the wide-angle X-ray diffraction patterns of Zn_2SiO_4:Mn samples obtained by both the mesoporous silica template (MST) and the conventional solid-state reaction (CSSR) methods and fired at various temperatures. In the diffraction pattern of the sample 8M-ZS(A) prepared by the MST method at 750 °C (Figure 1A,a), besides the peaks assigned to the reflections from the (101) and (002) planes of the ZnO phase, there are some other peaks observed. The positions of these peaks agree well with those of the standard pattern (No. 08-0492) reported by the Joint Committee on Powder Diffraction Standards (JCPDS) (shown in the inset of Figure 1A) for Zn_2SiO_4 in the phenacite structure (willemite). Indicatively, a crystalline Zn_2SiO_4 phase has formed at 750 °C by the MST method. No ZnO phase was detected by XRD, but only the well-defined diffraction pattern of the willemite phase was observed for the sample 8M-ZS(A) fired at 850 °C for 3 h, as shown in Figure 1A,b. Conventionally, the reaction between zinc oxide and silica proceeds with the primary reaction product being an amorphous orthosilicate complex before 775 °C, a firing time duration of over 140 h is required at 800 °C to produce as little as 10% crystalline zinc silicate, and only at 1200 °C or higher, a completely crystallized product can be obtained.[14] In this method, however, crystalline Zn_2SiO_4 could be obtained at 750 °C, and at 850 °C, only around 3 h was needed to produce fully crystallized willemite phosphor without detectable ZnO by XRD. This suggests that ZnO be reacted completely into Zn_2SiO_4 with Mn^{2+} dissolved throughout its lattice at 850 °C, and the slight excess amorphous silica, if any, has not been converted into quartz crystals yet. Thermodynamically, as compared with those of the silica used in the conventional method, the lower reaction temperature and quicker crystallization may be explained on the basis of the higher Gibbs free energy of the mesoporous silica,[15] due to its higher surface area and high-energy amorphous structure. The higher Gibbs free energy can effectively reduce the reaction activation energy and facilitate the reaction between silica and zinc oxide.

Although the peak positions of the phosphors prepared by the MST method are in good agreement with the standard pattern (JCPDS Card No. 08-0492) in Figure 1A, the relative intensities of the most intense peaks exhibit a shift. According to the standard pattern, the most intense peak should be the (410) peak with relative intensities of 100%, and a similar result was obtained for the reference sample CSSR, as shown in Figure 1A,c. In contrast, the maximum intensity in our samples prepared by the MST method is observed for the (113) peak. As reported previously,[11] there is some obvious preferred orientation in our samples. In the low-angle XRD patterns of the samples 0M-ZS, 8M-ZS(A), and 8M-ZS(N) prepared by the MST method and fired at 850 °C, as shown Figure 1B, a broad but clear diffraction peak, similar to the (100) characteristic peak

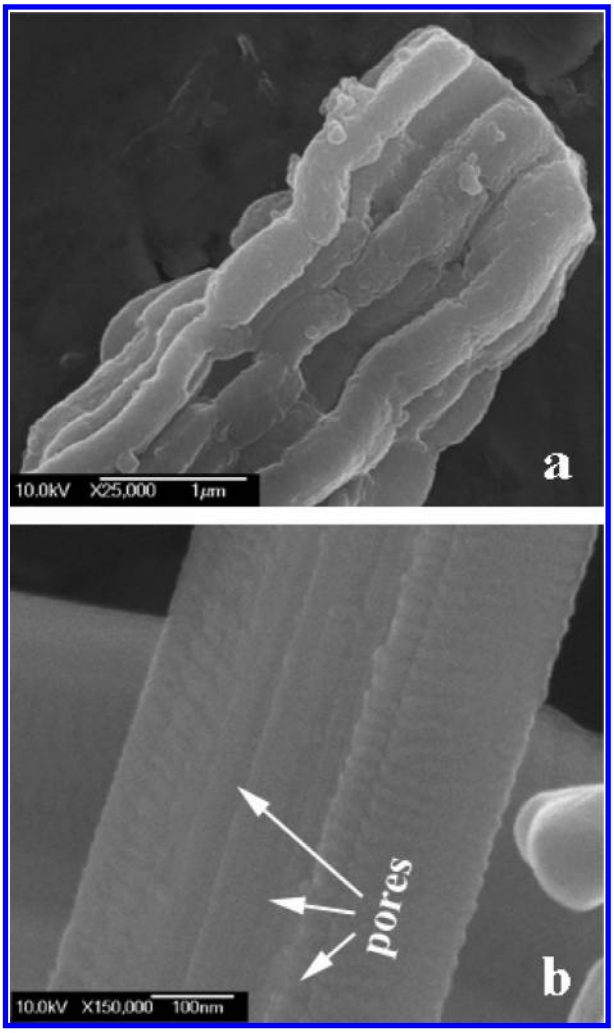

Figure 2. FE-SEM images of (a) the morphology of sample 8M-ZS(A) fired at 850 °C and (b) the profile of a ropelike particle in this sample.

of SBA-15 (shown in curve g of the inset in Figure 1B), was observed for all the samples, while only a straight line was observed for the reference sample CSSR (shown in curve h of the inset in Figure 1B). This implies a significant retention of the periodic structure though the ordered mesoporous silica SBA-15 template has almost completely converted into silicate.

Figure 2a shows the typical morphology of sample 8M-ZS(A) prepared at 850 °C, after it was treated with a 2 M NaOH aqueous solution. In this FE-SEM image, some elongated ropelike particles can be easily recognized and are morphologically similar to the active template SBA-15.[13] This implied that the phosphor product has inherited the structure and morphological characteristics of the template. In the profile view of one of the ropelike particles, as shown in Figure 2b, the particle is porous and some pore channels are retained inside the ropelike particle. However, the representative TEM image (Figure 3) of the sample 8M-ZS(A), taken at the top of a particle, does not display any pore channel opening outward, and N_2 sorption isotherms for all our samples (shown in Figure 4) are straight lines at a relative pressure P/P_0 of 0.1−0.8 instead of type IV isotherm curves, characteristic of SBA-15. Thus, the pore channels were closed inside the ropelike particle. Significantly, the particle is a single crystallite, which can be confirmed by the corresponding SAED pattern, as shown in the inset in Figure 3.

The proposed growth mechanism of the zinc silicate ropelike particle is shown in Figure 5. Zinc acetate and manganese

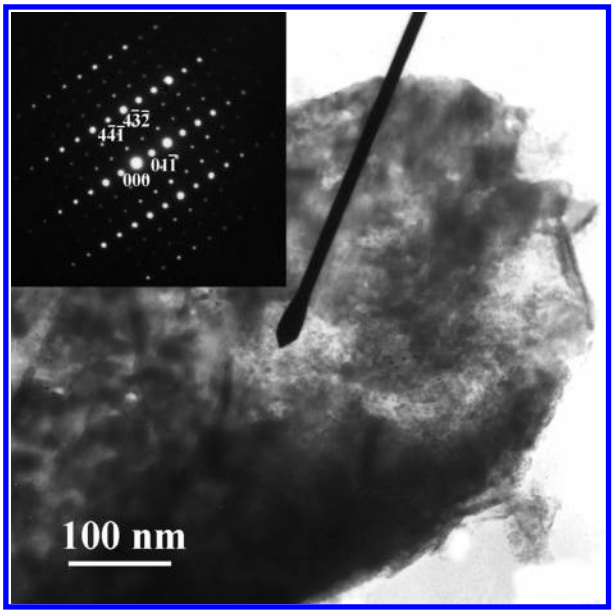

Figure 3. TEM image at the thin edge of a rod in sample 8M-ZS(A). Inset: related SAED pattern.

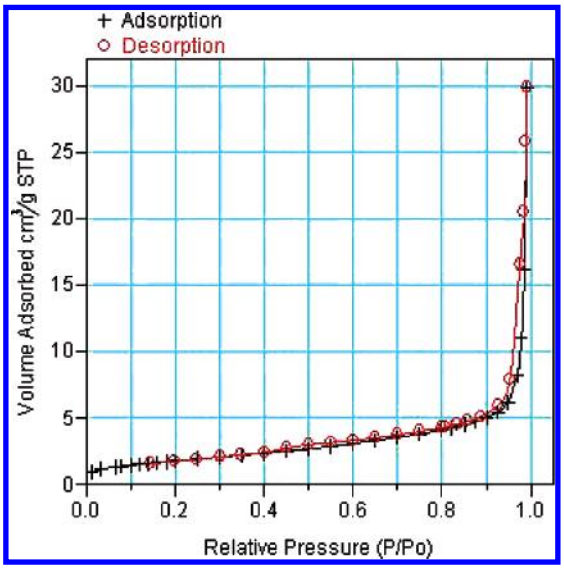

Figure 4. N_2 adsorption/desorption isotherms of sample 8M-ZS(A) fired at 850 °C.

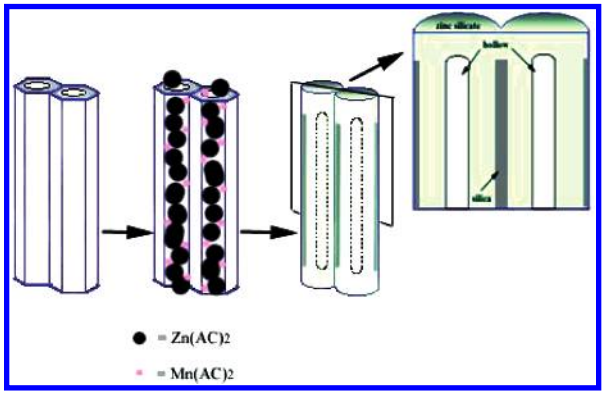

Figure 5. Proposed mechanism for the formation of Zn_2SiO_4 ropelike particles with closed pores using the mesoporous silica SBA-15 template.

acetate are supported on the framework of SBA-15 after the ethanol solvent is volatilized, and at the early calcination stage, the acetates are pyrolyzed into metal oxides. The formed zinc

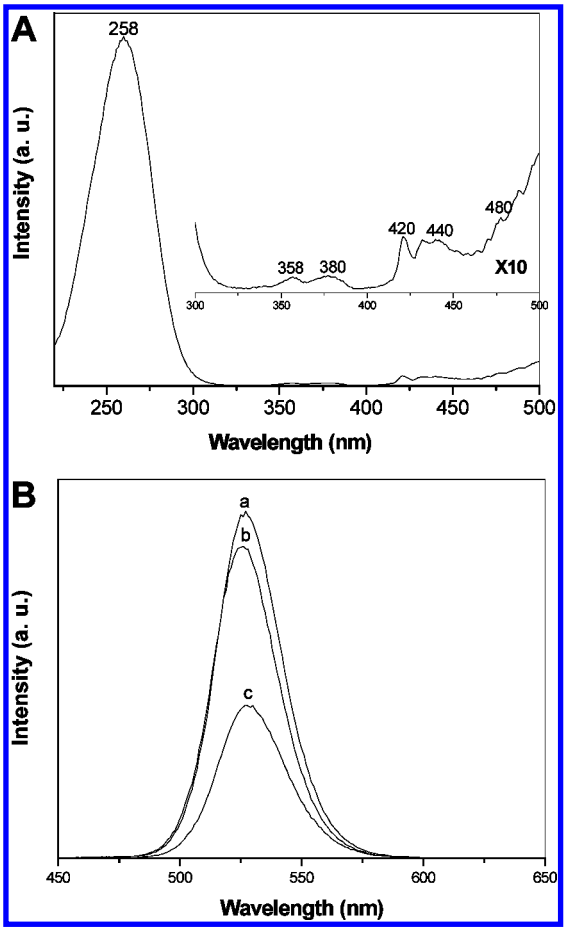

Figure 6. (A) Excitation spectrum (λ_{em} = 526 nm) of sample 8M-ZS(A). (B) Emission spectra of (a) sample 8M-ZS(A), (b) sample 8M-ZS(N), and (c) the reference sample CSSR under an excitation-light wavelength of 258 nm.

and manganese oxides are also adsorbed on the framework of SBA-15, and as the firing temperature increases, zinc oxide can react with the amorphous silica framework to form willemite seeds in the mesochannels. The reaction can be facilitated by the large surface area and high-energy amorphous framework of SBA-15. The seeds would grow along the ordered silica framework and then be arranged in an elongated morphology. Moreover, owing to the tendency of metal oxides to aggregate at the channel orifice, the coarse willemite crystal would further grow up only to seal the channel openings. That is why no capillary condensation and evaporation took place in N_2 absorption and desorption curves, and the N_2 sorption isotherms for all our samples are the straight lines at a relative pressure P/P_0 of 0.1−0.8 instead of type IV isotherm curves.

It is generally recognized that the luminescent properties of phosphors depend on their pairticle size and shape. In this experiment, since the phosphors prepared by using SBA-15 as the active template exhibit elongated ropelike morphology with ordered mesostructures inside them, and these elongated particles are locally oriented, these results are believed to impact the quantum efficiency and enhance the photoluminescence intensity.

Figure 6A shows the room-temperature excitation spectra for sample 8M-ZS(A), obtained by monitoring the green emission wavelength at 526 nm and using appropriate filters. In the spectrum, the strong and broad excitation peak at 258 nm was ascribed to the strong dipolar e → t_2 transition of Mn^{2+} ion in willemite according to the theoretical results calculated by K. C. Mishra,[16] and was mainly assigned to excite the green

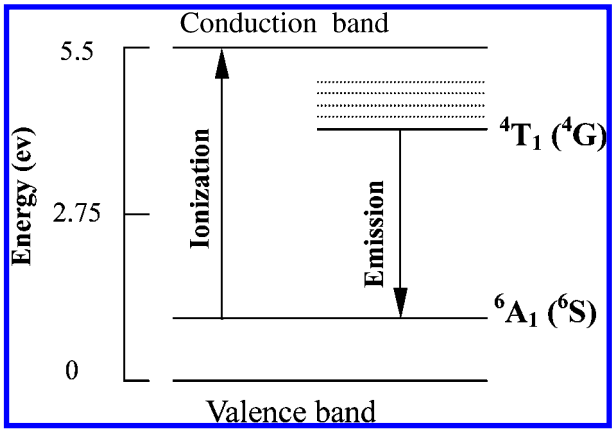

Figure 7. Energy level scheme describing the green light emission process for $Zn_2SiO_4:Mn^{2+}$ phosphor under an excitation-light wavelength of 258 nm.

luminescence. Other various bands due to the Mn^{2+} transitions are observed around 360, 380, 420, 440, and 480 nm, which result from the splitting of the ^4D and ^4G levels due to the crystalline field, according to the Orgel diagram of the Mn^{2+} ion.[5,17] The room temperature photoluminescence (PL) spectra for samples 8M-ZS(A) and 8M-ZS(N) and the reference sample CSSR are shown in Figure 6B under the excitation at 258 nm and by using appropriate but identical filters. The light emissions of all the samples peak at around 526 nm, and are ascribed to the electronic transition of $^4T_1(^4G) \rightarrow {}^6A_1(^6S)$ associated with Mn^{2+} ions in willemite.[18−20] The green emission mechanism can be referred to the process schematically shown in Figure 7: the electrons at the $^6A_1(^6S)$ ground state of Mn^{2+} ions, originated from the photoexcited ionization of Mn^{2+} ions, are excited to the conduction band (CB) of Zn_2SiO_4 by photons, and the free electrons in the CB can relax to the $^4T_1(^4G)$ excited state through a nonradiative process. This is followed by radiative transitions from the $^4T_1(^4G)$ excited state to the $^6A_1(^6S)$ ground state accompanied by green emission at 526 nm. Significantly, the relative PL intensities of samples 8M-ZS(A) and 8M-ZS(N) are much stronger than that of the sample CSSR with the conventional solid-state reaction method. It is indicative that the luminescent properties of the Mn-doped zinc silicate phosphors prepared by the MST method at 850 °C were obviously enhanced, despite the much lower firing temperature than that (about 1250 °C) required in the conventional SSR method for the complete crystallization of phosphors. For the phosphor products at the same doping level but prepared by different methods, the more homogeneously the Mn^{2+} ions are distributed in Zn_2SiO_4, the stronger the emission the phosphor will have, because concentration quenching takes place even at very low concentration when the distribution of the Mn^{2+} ions in Zn_2SiO_4 is inhomogeneous.[21] More homogeneous distribution of Mn^{2+} ions is achieved in the phosphor prepared by the MST method than that by the conventional SSR or other dry methods, owing to the high specific surface area, ordered mesochannels, and uniform thin silica wall of the mesoporous template. The mesochannels of the template facilitate Mn^{2+} ions to diffuse inside the particle and make them highly dispersive. Thus, the enhanced luminescence of the phosphor products prepared by the MST method can be well interpreted by the homogeneous distribution of Mn^{2+} ions.

Mn-doped Zn_2SiO_4 has been investigated extensively in terms of the manganese concentration. Recently, the effect of the manganese concentration on decay behavior has been a major concern.[5,19] Figure 8 represents the decay curves of $Zn_{2-x}Mn_xSiO_4$ phosphors, as a function of the manganese concentration *x*, and

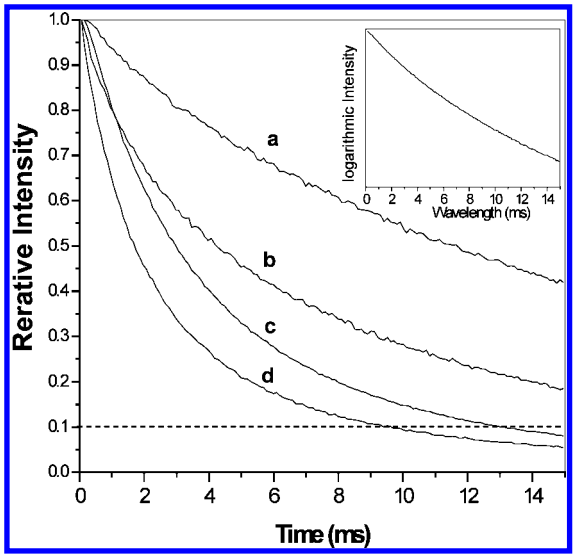

Figure 8. Decay curves of $Zn_{2-x}Mn_xSiO_4$ phosphors with manganese doping levels of (a) 0.02, (b) 0.05, (c) 0.08, and (d) 0.12 at $\lambda_{ex} = 258$ nm (Xe flash lamp). Inset: natural logarithmic intensity curve as a function of the decay time in (c).

its inset gives the natural logarithmic intensity curve as a function of the decay time of 8M-ZS(A). In Figure 8, the decay time decreases as the manganese concentration increases, and in particular, the decay curves cannot be characterized using a single-exponential function. Similar results have been reported previously;[5,19] however, the decay time ($t_{10\%}$) of each of our samples is obviously longer than that of the reported phosphor at the same Mn doping level. Morell et al.[5] argued that the decrease of the decay time with an increase of manganese concentration is closely related to the concentration quenching. Ronda and Amrein[22] suggested that the exchange interaction between Mn^{2+} ions indeed brings on allowable optical transition between Mn^{2+} ion pairs and further results in a shortening of the decay time at relatively high manganese concentration. The longer decay time was also expected to be due to the homogeneous distribution of Mn^{2+} ions and the closed pore structures, which are favorable in achieving uniform dispersion of Mn^{2+} ions and keeping the inter-ion ($Mn^{2+}-Mn^{2+}$) distance large enough.

Conclusions

We have proposed a facile route for preparing green light emitting Zn_2SiO_4:Mn phosphor via a low-temperature solid-state reaction method by using mesoporous silica SBA-15 as an active template. Combined structural and morphological characterizations show that the as-prepared Zn_2SiO_4:Mn phosphor has been well crystallized at 850 °C and inherited an ordered mesostructure as well as the macroscopic ropelike morphology of the parent template SBA-15. The profile SEM analysis demonstrates that pore channels have been closed inside the single-crystalline phosphor particle. Room temperature photoluminescence and decay kinetics of the phosphors show their strongly enhanced green emission and non-single-exponential decay behavior with a long decay time. The results strongly suggest that this route exhibits a significant advance in facilitating homogeneous doping, enhancing the luminescent properties of the Zn_2SiO_4:Mn phosphor and lowering the firing temperature. It should be emphasized that the concept of using mesoporous silica as an active template in the synthesis of silicate crystals with an oriented microstructure may be applicable to many other different silicate systems or a certain silicate system with different dopants to obtain remarkable optical properties and broader applications, owing to homogeneous distribution of doping ions and the low solid-state reaction temperature.

Acknowledgment. This work was supported by the National Natural Science Foundation of China (Grant No. 50232050), the National Hi-Tech Project of China (Grant No. 2002AA321010), Shanghai Sci. & Tech. Committee (Grant No. 03DJ14004), and the National Foundation Research Project (Grant No. 2002CB613305).

References and Notes

(1) (a) Kresge, C. T.; Leonowicz, M. E.; Roth, W. J.; Vartuli, J. C.; Beck, J. S. *Nature* **1992**, *359*, 710. (b) Beck, J. S.; Vartuli, J. C.; Roth, W. J.; Leonowicz, M. E.; Kresge, C. T.; Schmitt, K. D.; Chu, C. T.-W.; Olson, D. H.; Sheppard, E. W.; McCullen, S. B.; Higgins, J. B.; Schlenker, J. L. *J. Am. Chem. Soc.* **1992**, *114*, 10834. (c) Huo, Q.; Margolese, D. I.; Ciesla, U.; Feng, P.; Gier, T. E.; Sieger, P.; Leon, R.; Petroff, P. M.; Schüth, F.; Stucky, G. D. *Nature* **1994**, *368*, 317. (d) Tanev, P. T.; Pinnavaia, T. J.; *Science* **1995**, *267*, 865. (e) Corma, A. *Chem. Rev.* **1997**, *97*, 2373. (f) Shin, H. J.; Ryoo, R.; Liu, Z.; Terasaki, O. *J. Am. Chem. Soc.* **2001**, *123*, 1246. (g) Tian, B.; Liu, X.; Solovyov, L. A.; Liu, Z.; Yang, H.; Zhang, Z.; Xie, S.; Zhang, F.; Tu, B.; yu, C.; Terasak, O.; Zhao, D. *J. Am. Chem. Soc.* **2004**, *126*, 865.

(2) (a) Zhang, L.-X.; Shi, J.-L.; Yu, J.; Hua, Z.-L.; Zhao, X.-G.; Ruan, M.-L. *Adv. Mater.* **2002**, *14*, 1510. (b) Zhang, W.-H.; Shi, J.-L.; Wang, L.-Z.; Yan, D.-S. *Chem. Mater.* **2000**, *12*, 1408. (c) Li, L.; Shi, J.-L.; Zhang, L.-X.; Xiong, L.-M.; Yan, Y.-N. *Adv. Mater.* **2004**, *16*, 1079.

(3) Hu, B.; Shi, J. *J. Mater. Chem.* **2003**, *13*, 1250.

(4) Li, Q.; Brown, S. E.; Broadbelt, L. J.; Zheng, J.-G.; Wu, N. Q. *Micropor. Mesopor. Mater.* **2003**, *59*, 105.

(5) (a) Morell, A.; Khiati, N. El. *J. Electrochem. Soc.* **1993**, *140*, 2019. (b) Barthou, C.; Benoit, J.; Benalloul, P.; Morell, A. *J. Electrochem. Soc.* **1994**, *141*, 524.

(6) (a) Rack, P. D.; Naman, A.; Holloway, P. H.; Sun, S. S.; Tuenge, R. T. *Mater. Res. Soc. Bull.* **1996**, *21*, 49. (b) Copeland, T. S.; Lee, B. I.; Qi, J.; Elrod, A. K. *J. Lumin.* **2002**, *97*, 168.

(7) (a) Thilulouse, P.; Giess, E. A.; Chang, I. F. *J. Appl. Phys.* **1982**, *53*, 9015. (b) Cich, M.; Kim, K. *Appl. Phys. Lett.* **1998**, *73*, 2116.

(8) Kandarakis, I.; Cavouras, D.; Prassopoulos, P.; Nomicos, C. D.; Panayiotakis, G. S. *Appl. Phys. A* **1998**, *67*, 521.

(9) Stevels, A. L. N.; Vink, A. T. *J. Lumin.* **1974**, *8*, 443.

(10) Chang, I. F.; Brownlow, J. W.; Sun, T. I.; Wilson, J. S. *J. Electrochem. Soc.* **1989**, *136*, 3532.

(11) (a) Li, Q. H.; Komarneni, S.; Roy, R. *J. Mater. Sci.* **1995**, *30*, 2358. (b) Ahmadi, T. S.; Haase, M.; Weller, H. *Mater. Res. Bull.* **2000**, *35*, 1869.

(12) (a) Reybaud, L.; Broca-Cabarreq, C.; Mosset, A.; Ahamdance, H. *Mater. Res. Bull.* **1996**, *31*, 1133. (b) Morimo, R.; Monchinaga, R.; Nakamura, K. *Mater. Res. Bull.* **1994**, *29*, 751.

(13) Zhao, D.; Feng, J.; Huo, Q.; Melosh, N.; Fredrickson, G. H.; Chmelka, B. F.; Stucky, G. D. *Science* **1998**, *279*, 548.

(14) Froelich, H. C. *J. Phys. Chem.* **1943**, *47*, 669.

(15) Mohanty, P.; Ram, S. *Mater. Lett.* **2002**, *53*, 287.

(16) Mishra, K. C.; Johnson, K. H.; DeBoer, B. G.; Berkowitz, J. K.; Olsen, J.; Dale, E. A. *J. Lumin.* **1991**, *47*, 197.

(17) Orgel, L. E. *J. Chem. Phys.* **1955**, *23*, 1004.

(18) (a) Perkins, H. K.; Sienko, M. J. *J. Chem. Phys.* **1967**, *46*, 2398. (b) Palunbo, D. T.; Brown, J. J., Jr. *J. Electrochem. Soc.* **1970**, *117*, 1184.

(19) Sohn, K.-S.; Cho, B.; Park, H. D. *J. Am. Ceram. Soc.* **1999**, *82*, 2779.

(20) (a) Sun, X. W.; Kwok, H. S. *Appl. Phys. A* **1999**, *69* (Suppl.), S39. (b) Selomuly, R.; Ski, S.; Pita, K.; Kam, C. H.; Zhang, Q. Y.; Buddhudu, S. *Mater. Sci. Eng., B* **2003**, *100*, 136.

(21) Morimo, R.; Matae, K. *Mater. Res. Bull.* **1989**, *24*, 175.

(22) Ronda, C. R.; Amrein, T. *J. Lumin.* **1996**, *69*, 245.